Journal of Power Sources 215 (2012) 160–163

Contents lists available at SciVerse ScienceDirect

Journal of Power Sources

journal homepage: www.elsevier.com/locate/jpowsour

Short communication

Compositional control of continuously graded anode functional layer

J. McCoppin*, I. Barney, S. Mukhopadhyay, R. Miller, T. Reitz, D. Young

Wright State University, 3640 Colonel Glenn Hwy., Dayton, OH 45435, USA

HIGHLIGHTS

- SOFC compositionally graded AFL built using a duel suspension spraying system.
- Analytical deposition model predicted and matched elemental gradation of the functional layer.
- Deposition profile/thickness significantly affects the electrochemical kinetics.
- Supports model that indicates effectively grading the AFL improves SOFC performance.

ARTICLE INFO

Article history:
Received 3 March 2012
Received in revised form
8 May 2012
Accepted 11 May 2012
Available online 17 May 2012

Keywords:
Solid oxide fuel cell
Anode
Spray deposition
Compositional gradation
SOFC

ABSTRACT

In this work, solid oxide fuel cells (SOFC's) are fabricated with linear-compositionally graded anode functional layers (CGAFL) using a computer-controlled compound aerosol deposition (CCAD) system. Cells with different CGAFL thicknesses (30 um and 50 um) are prepared with a continuous compositionally graded interface deposited between the electrolyte and anode support current collecting regions. The compositional profile was characterized using energy dispersive X-ray spectroscopic mapping. An analytical model of the compound aerosol deposition was developed. The model predicted compositional profiles for both samples that closely matched the measured profiles, suggesting that aerosol-based deposition methods are capable of creating functional gradation on length scales suitable for solid oxide fuel cell structures. The electrochemical performances of the two cells are analyzed using electrochemical impedance spectroscopy (EIS).

1. Introduction

Recent improvements in solid oxide fuel cell performance have come about through various strategies. Materials with improved electrochemical and catalytic performance as well as tailored microstructures show improved performance over previous SOFC designs [1–4]. In the area of tailored microstructure, composite electrodes provide a significant advantage to improve electrochemical performance [5]. Because of the improved electrochemical performance, the addition of an interlayer at the electrode/electrolyte interface has been the focus of much recent research [6]. Typically, the insertion of an interlayer decreases the activation polarization by effectively increasing triple phase boundaries [7]. Of special interest is the incorporation of an interlayer by means of gradation to functionally transition from electrode to electrolyte [8,9]. Typical gradation schemes include continuous compositional gradation, as well as porosity gradation and grading the ratio of the electrode/electrolyte particle size [10]. However, the exact effects that continuously graded layers have upon fuel cell performance remains an open question. Computational modeling by Schneider et al. argues that graded electrodes do not significantly perform better than an optimized randomly mixed composite electrode [11]. On the contrary, modeling by Chen et al. argues that effective gradation using precise composition deposition control is required to avoid non-percolating compositions within the functional layer, and would result in a significant advantage over randomly mixed composite electrodes [12]. While experimental results on functionally graded SOFC structures are needed in order to validate these hypotheses, traditional fabrication methods such as tape casting and screen-printing are stepwise processes that lack the necessary flexibility and fidelity. Recently, aerosol-based deposition methods (CCAD) have been used to fabricate functionally graded SOFC cathode interlayers using in-situ, computer adjustment of the deposition composition [13].

In this work, the CCAD system was used to fabricate SOFC structures with functionally graded anode layers. The resulting cells were structurally and compositionally characterized with scanning electron microscopy (SEM) and Energy Dispersive Spectroscopic

* Corresponding author. Tel.: +1 937 238 9700; fax: +1 937 775 5082.
E-mail addresses: mccoppin.3@wright.edu, jmccoppin@hotmail.com (J. McCoppin).

0378-7753/$ – see front matter © 2012 Elsevier B.V. All rights reserved.
doi:10.1016/j.jpowsour.2012.05.024

(EDS) mapping techniques, in order to determine if this deposition method is suitable for precise control of functional gradation in SOFC structures. Electrochemical performance is analyzed using impedance spectroscopy to compare the relative effect of gradation layer thickness on the impedance and power densities of the two cells.

2. Experimental

Anode substrates were fabricated by uniaxial pressing [14,15]. A base anode powder was prepared using a combination of 55 wt% Nickel Oxide (Aldrich) and 45 wt% YSZ (TZ-8Y, Tosoh-Zirconia). The base powder was ball milled in ethanol for 24 h to ensure even distribution of both materials and then pressed into pellets. The substrates were subsequently bisque fired in air at 900 °C for 1 h. Anode, cathode and electrolyte inks were prepared for cell fabrication. The formulation of the inks included dispersants, plasticizers, and binders, followed by homogenization to stabilize the solution. Particle dispersion was achieved, via the steric method, with addition of butyl benzyl phthalate (BBP) followed by ball milling for 24 h. Stabilization of the solution required the addition of polyvinyl butyral (PVB, B-98) as a binder and polyalkylene glycol (PAG) as a plasticizer, followed by ball-milling for an additional 24 h prior to deposition. The solids loading of each ink was 3.35, 3.77, and 0.74 vol.% for the YSZ, NiO, and LSM powders respectively. Each ink consisted of its respective powder with 0.39 g of PAG, BBP, PVB each, in 50 ml of ethanol.

For this research, the CCAD system used a linear gradation algorithm to deposit two CGAFL's. The two inks used for anode gradation contained 3.77% NiO and and 3.35% YSZ solids loading (by volume) respectively, resulting in approximately 1:0.9 volume fraction ratios. The details of the method for depositing the CGAFL using the CCAD system is described elsewhere [13]. Two cells were fabricated by this technique in order to examine the effects of interlayer thickness on composition control while maintaining the same linearly graded profile. To achieve an even coverage using aerosol deposition, a fraction of the substrate rotated at 100rpm under the spray cone. Graded deposition occurred at a rate of 30 ml h^{-1} for 1 min (Cell 1) and 2 min (Cell 2) with all other variables left consistent. This resulted in the formation of approximately 30 and 50um CGAFL's. Each cell subsequently received constant deposition of electrolyte ink at 30 ml h^{-1} for 1 min via the CCWPS onto the as-deposited CGAFL forming approximately 30um electrolyte layers. Co-sintering was then performed at 1400 °C for 5 h to produce a dense, crack-free electrolyte atop the anode electrode. After sintering, cathode ink was deposited at 30 ml h^{-1} for 2 min via CCAD and was sintered at 1200 °C for 2 h, resulting in a 20 um thick layer.

Energy dispersive spectroscopy analysis was performed using an Ametek EDAX unit, operated by Genesis 5.1 software on a JEOL 7401-FE-SEM scanning electron microscope. EIS was performed using an EG&G model 274 potentiometer. Electrochemical testing of each cell was preformed at 650, 750, and 850 °C. The specific preparation methods and testing procedures have been discussed previously [13].

3. Theory and calculation

The functional layer is located between the electrode and electrolyte interface to facilitate the electrochemical reaction of the SOFC. Tailoring of the gradation profile of the functional layer can aid in this electrochemical reaction [16]. CCAD allows for tailored functional layer profiles. The combined time-dependent deposition of electrode and electrolyte inks determines the composition profile of the functional layer. To achieve an optimally graded interlayer profile, a deposition algorithm should allow for the deposition of a CGAFL that allows for both effective percolation of the charge carrying species and functionally grading the composition of the electrode and electrolyte, in order to meet the increasing and decreasing electrochemical demands of the disparate charge carriers [12]. The cross flux of the electron and ion charge carrying species use fundamentally different transport mechanisms. Effective modeling and empirical studies are required to determine the most effective profile to optimize a mutual cross flux [11]. To maintain continuous electronic and mass transport characteristics into and out of the functional layer, the initial deposition rates of the two inks should initiate a CGAFL that matches the support substrate composition and end with deposition rates that finalize the CGAFL with an effective electron percolation threshold at the electrolyte. The percolation threshold is a function of particle size ratio, particle concentration, and other variables that render it difficult to estimate [12]. The CGAFL in this work ends at 100% electrolyte composition, and followed a linear gradation profile.

In this profile, the combined flow rate ψ of the two inks remained constant. Throughout the total deposition time$T$, the flow rate of the electrolyte ink continuously increased while the flow rate of the anode ink complementarily decreased. The flow rate of the solid electrolyte ε and anode α material in the atomized ink as a function of time (t) in seconds is

$$\varepsilon(t) = \frac{\chi_\varepsilon \psi}{2}\left(1 + \frac{t}{T}\right) \tag{1}$$

and

$$\alpha(t) = \frac{\chi_\alpha \psi}{2}\left(1 - \frac{t}{T}\right) \tag{2}$$

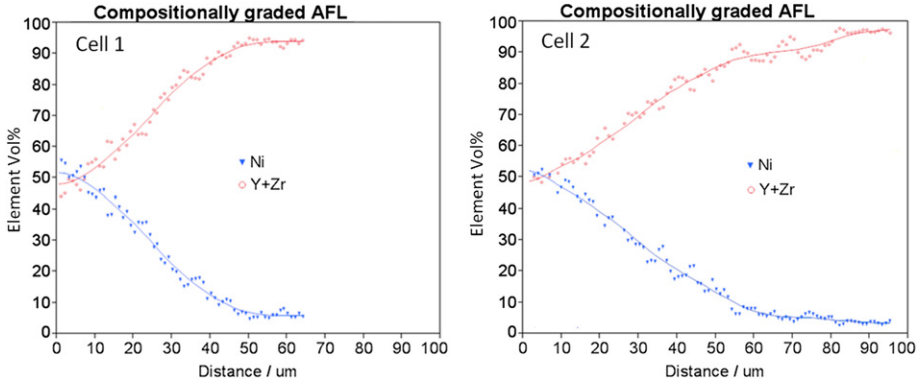

Fig. 1. Profile plots of the two CGAFL's identify the volume fraction as a function of layer thickness.

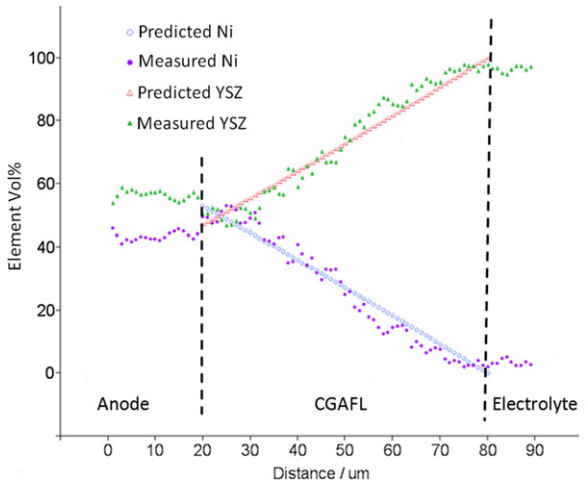

Fig. 2. Profile plots showing comparison of predictive model with experimental data collected from cell 1.

where χ_α and χ_ε are the volume fractions of solid material in the respective ink. Combining equations (1) and (2) and integrating gives the total amount of solid material θ deposited over time.

$$\theta = \frac{\psi t}{2}\left(\chi_\alpha - \frac{\chi_\alpha t}{2T} + \chi_\varepsilon + \frac{\chi_\varepsilon t}{2T}\right) \tag{3}$$

Dividing equation (2) by the derivative of equation (3), followed by parameterizing with equation (3) by time, allows pairing the concentration of anode material y with its respective linear position x (taking into account geometry), given by:

$$x = \frac{\psi T((-1+y)\chi_\alpha + y\chi_\varepsilon)((-1+y)\chi_\alpha^2 - 3\chi_\alpha\chi_\varepsilon - y\chi_\varepsilon^2)}{4(\chi_\alpha - y\chi_\alpha + y\chi_\varepsilon)^2} \tag{4}$$

Controlling the resulting volume fractions of solid material within the CGAFL as a function of combined flow rates requires consideration of χ for each ink. Deposition of inks with different χ values renders the resulting gradation profile nonlinear. Solving equation (4) with different values of χ illustrates the significant effect that volume fraction of solid material in the two inks has on the accuracy of matching the linear gradation algorithm. This is important to note because the volume fraction of solid material within an ink may not be an easily-controlled parameter. Therefore,

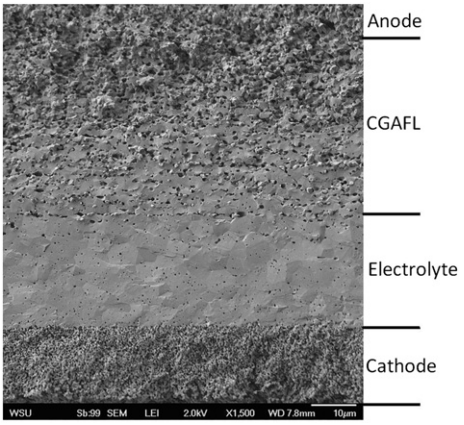

Fig. 3. SEM of SOFC having a CGAFL illustrating the engineered microstructure.

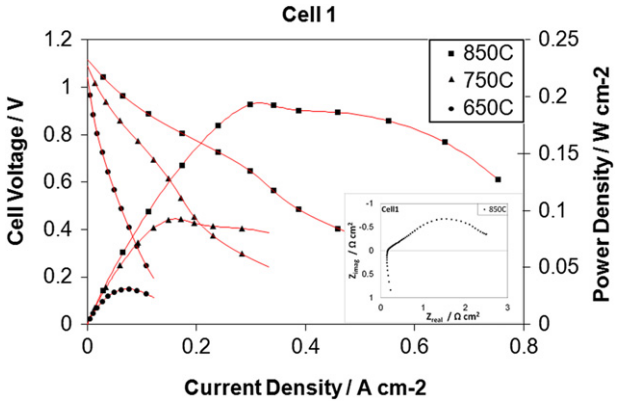

Fig. 4. *I–V*, power density and impedance spectra curves of cell 1.

the resulting deposition profile of the CGAFL is not only a function of deposition time and ink flow rates, but also the χ values of the inks. In order to achieve the highest algorithm matching accuracy, the two χ values of the electrode and electrolyte inks should be as close to equal as possible.

4. Results and discussion

EDX maps were taken over an area that included the electrode, interlayer (CGAFL) and the electrolyte. The resulting line-by-line volume percent data from the maps was averaged and converted into *X–Y* scatter plots, shown in Fig. 1. The plots display the elemental volume percent as a function of position to plot the "averaged" gradation of the profile. The plots are effective at identifying the CGAFL's thickness, and can be used to identify the thickness of the CGAFL's profile that resides in non-percolating regions if the cutoff values are known. The analytical model developed in the previous section, accounting for the specific deposition parameter values, allowed for the generation of predictive plots to evaluate the collected data. The effective continuous stream of solid material, deposited onto the substrate, resulted from a fractional spray–cone interaction and other substrate–aerosol interactions. Using the diameter of the substrate and applying the fractional and geometric factors to equation (3) allowed for calculation of layer thickness as a function of time. Fractionalizing and then parameterizing equations (1) and (2) separately with the adjusted equation (3) provided predictive plots of the CGAFL profile seen in Fig. 2.

Scanning electron microscopy was used to provide detailed observation of the microstructure. Fig. 3 is a micrograph of cell 2

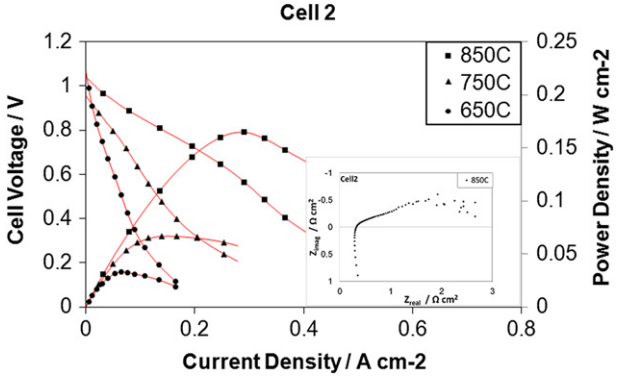

Fig. 5. *I–V*, power density and impedance spectra curves of cell 2.

showing detailed spatial distribution of the nickel within the YSZ as it grades toward the solid electrolyte. Isolated electrode regions close to the electrolyte are apparent in the micrograph.

Polarization curves were taken at a rate of 0.1 V per minute, allowing for cell equilibrium between current collections. Figs. 4 and 5 show the polarization data for Cell 1 and Cell 2 respectively. The maximum power density at 850 °C of cell 1, having the thinner CGAFL, and cell 2, having the thicker CGAFL, is 195 mW cm^{-2} and 165 mW cm^{-2} respectively. A control cell, fabricated by using the same pressed substrate and comparable cathode deposition as the two CGAFL cells but without a CGAFL, exhibits a power density of 108 mW cm^{-2} at 850 °C. When comparing the CGAFL cells to the control, the polarization graphs indicate that there is a relative benefit to the addition of a linear CGAFL deposited by the CCWPS. It can also be determined that increasing the thickness of the linear CGAFL has a diminishing effect on the overall performance. One possible explanation for this decrease in performance is that the linear compositional profile contains regions that are below the electrical percolation threshold. This effect, as evident in Fig. 3, is just above the line on the right-hand side indicating demarcation of the electrolyte. As the CGAFL increases in thickness, this region also expands. This data suggests that further investigation into nonlinear CGAFL profiles may be beneficial to cell performance.

Energy impedance spectroscopy was performed at 850 °C, from 0.1 Ω to 100 kΩ, in order to allow further comparison of electrical performance. Figs. 4 and 5 show the Nyquist plots of cells 1 and 2 in the lower corner. The diminishing effect of the increased CGAFL layer thickness becomes apparent when comparing the impedance of the Nyquist plots. When comparing the two graphs, it can be seen that the initial arch, associated with high frequency region wherein charge transport and redox reactions dominate, is depressed and elongated in Cell 2. The elongation indicates an increase in area specific ohmic resistance (ASOR) brought about possibly by resistance to ionic conduction.

Using the discrete element method (DEM) modeling, Schneider et al. evaluates the performance of both a functionally graded composite electrode and a uniformly randomly mixed composite electrode. In their work, they indicate that although the optimized, uniformly randomly mixed composite electrode has slightly higher triple phase density, the functionally graded composite electrode exhibited slightly better effective electrode conductivity. Schneider et al. implied that the improved electrode conductivity results from a strong ionic network brought about by an increase volume fraction of ionic particles, while maintaining electronic percolation between the current collector and the electrolyte. The two cells fabricated in this work may support the results of this computational work. Cell 1 and 2 both demonstrate significant performance enhancement compared to the control cell without an interlayer, but it is apparent that the performance of Cell 1 was higher than that of Cell 2. According to the computational modeling work by Schneider et al. and the results from this work showing precise deposition control seen in Fig. 3, compositionally graded electrodes are a viable method of increasing performance of SOFC's.

5. Conclusion

In this research, CGAFLs were fabricated using the CCAD deposition technique. Characterization using SEM and EDX mapping of the CGAFL confirmed the tailored microstructure and composition. A predictive model of the deposition process was developed and the compositional profile indicated by the EDX maps matched well with the model. Electrochemical of the two cells provides evidence that the graded compositional profile can have a strong effect on electrochemical performance. Future optimization efforts may benefit from the use of CCAD, or similar aerosol-based processes, since it provides an effective method for tailoring the compositional profile of an electrode functional layer in a highly controlled manner.

References

[1] J. Fergus, R. Hui, X. Li, W.P. David, J. Zhang, Solid Oxide Fuel Cells: Materials Properties and Performance, CRC Press, Boca Raton, 2009.
[2] C. Sun, R. Hui, J. Roller, Journal of Solid State Electrochemistry 14 (2009) 1125–1144.
[3] A.J. Jacobson, Chemistry of Materials 22 (2010) 660–674.
[4] N.H. Menzler, F. Tietz, S. Uhlenbruck, H.P. Buchkremer, D. Stöver, Journal of Materials Science 45 (2010) 3109–3135.
[5] M. Mogensen, S. Primdahl, M.J. Jérgensen, C. Bagger, Journal of Electroceramics (2000).
[6] A.V. Virkar, J. Chen, C.W. Tanner, J.-woh Kim, Solid State Ionics 131 (2000) 189–198.
[7] K. Chen, X. Chen, Z. Lu, N. Ai, X. Huang, W. Su, Electrochimica Acta 53 (2008) 7825–7830.
[8] Z. Wang, N. Zhang, J. Qiao, K. Sun, P. Xu, Electrochemistry Communications 11 (2009) 1120–1123.
[9] J. Kong, K. Sun, D. Zhou, N. Zhang, J. Mu, J. Qiao, Journal of Power Sources 166 (2007) 337–342.
[10] A.C. Mu, D. Herbstritt, E. Ivers-tiffe, Solid State Ionics 153 (2002) 537–542.
[11] L. Schneider, C. Martin, Y. Bultel, L. Dessemond, D. Bouvard, Electrochimica Acta 52 (2007) 3190–3198.
[12] D. Chen, Z. Lin, H. Zhu, R.J. Kee, Journal of Power Sources 191 (2009) 240–252.
[13] J. McCoppin, D. Young, T. Reitz, A. Maleszewski, S. Mukhopadhyay, Journal of Power Sources 196 (2011) 3761–3765.
[14] D. Lee, Solid State Ionics 166 (2004) 13–17.
[15] K.G. Ewsuk, J.G. Argüello, Key Engineering Materials 264-268 (2004) 149–154.
[16] N.T. Hart, N.P. Brandon, M.J. Day, N. Lapen, Journal of Power Sources 106 (2002) 42–50.